DPSK Signals Demodulation Based on a Graded-index Multimode Fiber Mismatch Spliced between Two Single-mode Fibers

Xiaoyong Chen and Paloma R. Horche
Departamento de Tecnología Fotónica y Bioingeniería, Universidad Politécnica de Madrid, Avda. Complutense 30, Madrid, Spain

Keywords: Optical Fiber Communication, Optical Receiver, Differential Phase Shift Keying, Multimode Fiber, Modal Interference, Mach-Zehnder Interferometer.

Abstract: Differential phase shift keying (DPSK) signal has been shown as a robust solution for next-generation optical transmission systems. One key device enabling such systems is the delay interferometer, converting a phase signal into an intensity modulated signal to be detected by a photodiode. Usually, a Mach-Zehnder interferometer (MZI) is used for DPSK signals demodulation. In this work, we develop an alternative all-fiber MZI, which is based on a graded-index multimode fiber (MMF) mismatch spliced between two single-mode fibers. Interferometer performance is analyzed through both theory and experiment. Experimental results of transmission spectrums show that interference extinction ratio as high as 18 dB is obtained. Finally, we demonstrate, through simulation, that our proposed all-fiber MZI can be used for DPSK signals demodulation. Receiver sensitivity of -22.5 dBm at a bit error rate of 10^{-15} is obtained in the simulation for detecting a 40 Gbps DPSK signal, which is 1.3±0.2 dB penalty compared to the conventional receiver.

1 INTRODUCTION

Differential Phase Shift Keying (DPSK) signal, which encodes the binary data as either a 0 or π optical phase shift between the adjacent bits, has been proposed for using in optical transmission systems, since it exhibits superior optical signal to noise ratio (OSNR) sensitivity, high tolerance to chromatic dispersion and high robustness to fiber nonlinear effects (Gnauck and Winzer, 2005; Winzer and Essiambre, 2006). Compared with the on-off keying (OOK), the most obvious benefit of DPSK is the ~ 3-dB OSNR improvement to reach a given BER. Such advantage can be used to extend the transmission distance, reduce optical requirements, and relax component specifications. Note, however, that this ~ 3-dB benefit can only be obtained using balanced detection.

Usually, a conventional Mach-Zehnder interferometer (MZI) is used as the delay interferometer (DI) for DPSK signals demodulation, due to the simple structure and easy implementation. However, the conventional MZIs have one obvious drawback: the performance is easily affected by the environment, such as temperature, since two beams go through two different physical paths.

In order to improve the MZI performance, all-fiber MZI, which is based on a multimode fiber (MMF) located between two single-mode fibers (SMFs), is proposed to take place of the conventional MZI in recent years. Nowadays, all-fiber MZIs have been studied and developed to act as novel optical devices, e.g., a temperature sensor, a strain sensor, a refractive index sensor, a fiber lens, a bandpass filter, and a signal demodulator (Mohammed, Mehta and Johnson, 2004; Lize, Gomma and Kashyap, 2006; Tripathi et al., 2009; Tripathi et al., 2010; Wang at al., 2011; Xue and Yang, 2012; Hofmann et al., 2012; Shao et al., 2014). The principle of all-fiber MMF based MZIs is that, the optical power is coupled into two dominated modes, LP_{01} and LP_{02}, excited in the MMF, when light transmits from the input-SMF to the MMF; then, these two modes propagate along the MMF with different propagation constants, and interfere with each other when they transmit from the MMF to the output-SMF. Although some high-order modes are also excited and propagating in the MMF, they will not seriously affect the interference occurs between modes LP_{01} and LP_{02}. Therefore, such structure, SMF-MMF-SMF (SMS), can approximately work as a MZI. The main advantage of all-fiber MMF based MZI, compared to the conventional MZI, is low-cost, easy manufacture,

Chen X. and R. Horche P.
DPSK Signals Demodulation Based on a Graded-index Multimode Fiber Mismatch Spliced between Two Single-mode Fibers.
DOI: 10.5220/0005332500130019
In *Proceedings of the 3rd International Conference on Photonics, Optics and Laser Technology* (PHOTOPTICS-2015), pages 13-19
ISBN: 978-989-758-092-5
Copyright © 2015 SCITEPRESS (Science and Technology Publications, Lda.)

and performance improvement due to the two arms sharing the same hardware. However, the drawback of such MZIs is also obvious: the interference extinction ratio (ER) is very low, since the power coupled into mode LP_{01} is much higher than that coupled into the mode LP_{02}. In addition, the other high-order modes exited and propagating in the MMF will also affect the interference ER.

To improve the interference ER, some schemes, through using a special fiber to replace the commercial graded-index MMF in the SMS structure, have been proposed, including: a photonic crystal fiber (PCF) (Du et al., 2010), a double cladding fiber (Pang et al., 2009), a thin-core fiber (Zhu et al., 2010), and a graded-index MMF with a central dip (Chen, Horche and Minguez, 2014). In this work, we propose an alternative all-fiber MZI, which is a graded-index MMF mismatch spliced between two SMFs, as shown in Figure 1(a). With a transverse offset, more power is coupled into the first non-circular symmetrical mode LP_{11}, while less power is coupled into fundamental mode LP_{01}, resulting in balancing the power difference between two beating modes, and thus improving the interference ER. This improvement makes it possible to use for DPSK signals demodulation.

Some previous papers have studied the application of an all-fiber in-line MZI using as a DPSK demodulator, which includes a birefringent fiber based MZI (Chow and Tsang, 2005), a special step-index MMF based MZI (Lize, Gomma and Kashyap, 2006), a PCF based MZI (Du et al., 2010), and an all-fiber MZI based on a graded-index MMF with a central dip in index profile (Chen, Horche and Minguez, 2014). In this work, we propose an alternative DPSK receiver, which is based on our proposed all-fiber MZI. In comparison with the schemes mentioned above, our proposed DPSK receiver also shows merits of low-cost, easy manufacture and good performance.

The paper is organized as follows. The theory of the proposed all-fiber MZI is presented in Section 2. Experimental setup and results are presented and discussed in Section 3. DPSK receiver based on the proposed all-fiber MZI for 40 Gbps DPSK signals demodulation is presented, and simulation results are commented in Section 4. Finally, conclusions are drawn in Section 5.

2 THEORY

Figure 1(a) shows our proposed all-fiber MZI, which is based on a graded-index MMF mismatch spliced between two SMFs. Note that only the core fibers are drawn in this figure.

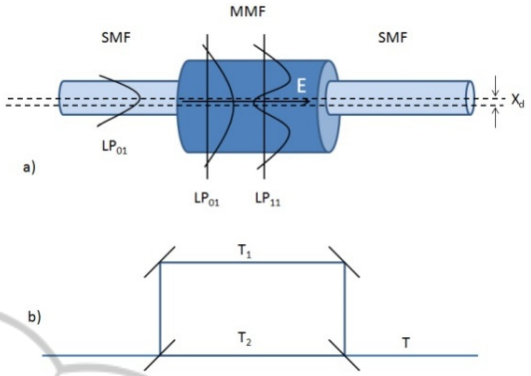

Figure 1: Principle of the proposed MZI (a) compared with the conventional MZI (b).

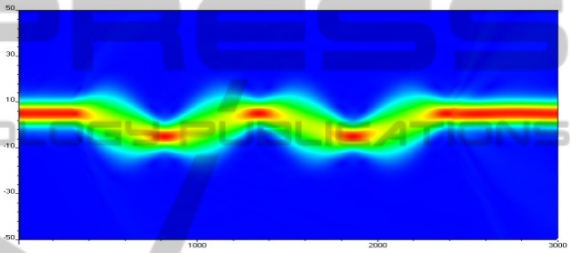

(a)

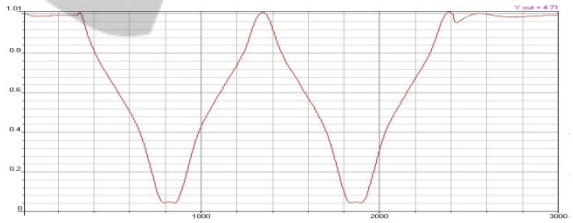

(b)

Figure 2: (a) Power distribution inside the graded-index MMF in the case of incident light offset from the MMF center (+5 μm); (b) Power distribution along the optical axis of +5 μm.

According to the theory of modal interference, which is a well-known phenomenon and it had been studied by many authors (Horche, Muriel and Pereda, 1989; Abe et al., 1992; Blahut and Kasprzak, 2004; Mohammed, Mehta and Johnson, 2004; Tripathi et al., 2009; Tripathi et al., 2010; Wang at al., 2011; Xue and Yang, 2012; Hof mann et al., 2012; Shao et al., 2014), the excited modes in the MMF interfere with each other along the propagation direction, and the power distribution along the propagation direction can be drawn as Figure 2(a). It can be seen that the power distributes periodically along the MMF, and almost all the power is coupled back to the output-SMF. Figure 2(b) shows the

corresponding power distribution along the propagation axis (+ 5μm). Defining the field distribution of each excited mode LP_{nk} as ψ_{nk}, and assuming that the transverse offset between the input-SMF and the MMF is x_d. Also, assuming that the output-SMF has the same parameters as the input-SMF and has the same transverse offset x_d, the power coupled into the output-SMF can be written as (Kumar et al., 2003):

$$P_{out} = \left| \int_0^{\infty} \psi(r,L) E_{in}^{*}(r - x_d) r dr \right|^2 = \left| \sum_{n=0}^{N} \sum_{k=1}^{K} c_{nk}^2 \exp(i(\beta_{01} - \beta_{nk})L) \right|^2 \quad (1)$$

where E_{in} is the normalized input field and $\psi(r,L)$ are the normalized eigenmode at the end of the MMF. c_{nk}^2 and β_{nk} are, respectively, the coupling coefficient and propagation constant of each excited mode in the MMF. The equation indicates that the power coupled into the output-SMF depends on the relative phase difference at the end of the MMF (L).

Although many modes are excited and propagating in the MMF, most of the power is coupled into modes LP_{01} and LP_{11}, due to the transverse offset between the input-SMF and the MMF. Therefore, our scheme can approximately work as a MZI. Also, since the power difference between these two modes is reduced much, compared to the SMS structure where the MMF is aligned to the SMFs, interference ER of our proposed MZI is improved. In addition, compared with the conventional MZI built with two fiber couplers, as shown in Figure 1(b), our proposed all-fiber MZI performs more stably, because both arms share the same hardware, resulting in less sensitive to the external environment, such as temperature. It should be noted that in the conventional MZI, the light is first split equally into two beams by a fiber coupler, and then they pass through two different physical paths. Finally, they re-combine together by another fiber coupler and interfere with each other due to the phase difference between two beams.

Despite a little power is coupled into some high-order modes, these modes do not seriously affect the transmission spectrum of our proposed all-fiber MZI. The only influence they generate is slightly changing the interference ER, leading to the outline of transmission spectrum periodically oscillating with the wavelength (or frequency), which is verified in Section 3. If we ignore the high-order modes excited in the MMF, the transmission function (Equation (1)) of our proposed all-fiber MZI can be simply expressed as that of a conventional MZI:

$$T = T_1 + T_2 + 2\sqrt{T_1 T_2}\cos(\varphi) \quad (2)$$

where T_1 and T_2 represent the intensity of modes LP_{01} and LP_{11}, respectively. φ is the phase difference between these two modes, and it can be written as:

$$\varphi = \int_0^L \Delta\beta\,(z)dz = L\Delta\beta \quad (3)$$

where L is the MMF length, $\Delta\beta$ is the propagation constants difference between modes LP_{01} and LP_{11}. In combination with (2) and (3), we can see that the power coupled into the output-SMF is only decided by the MMF length, L.

To concentrate the power on the axis location of the output-SMF at the end of the MMF, the phase difference between these two dominated modes should be equal to an integer multiple of 2π. In other words, the MMF length should be an integer multiple of beat length z_b, which can be written as:

$$z_b = \frac{2\pi}{|\beta_{01} - \beta_{11}|} \quad (4)$$

where β_{01} and β_{11} are the propagation constants of modes LP_{01} and LP_{11}, respectively.

The transmission spacing Δλ between the adjacent constructive peaks (or destructive valleys) can be written as:

$$\Delta\lambda = \frac{\lambda^2}{|n_{01} - n_{11}|L} = \frac{2\pi\lambda}{|\beta_{01} - \beta_{11}|L} = \frac{\lambda\, z_b}{L} \quad (5)$$

where n_{01} and n_{11} are the effective index of modes LP_{01} and LP_{11}, respectively. We can see that, according to (5), the spacing Δλ is inversely proportional to MMF length. In addition, the propagation constants difference between the two beating modes can be approximately written as (Horche et al., 1989):

$$\beta_{01} - \beta_{11} = \frac{\lambda}{4\pi a^2 n_{\text{core}}}(U_{01}^2 - U_{11}^2) \quad (6)$$

with

$U_{01} = 2.405\ e^{-1/V}$ for the mode LP_{01}

$U_{11} = 3.83\ e^{-1/V}$ for the mode LP_{11}

$$V = \frac{2\pi a}{\lambda}\sqrt{n_{core}^2 - n_{clad}^2}$$

where a is the core radius, λ is the wavelength in vacuum, n_{core} is the maximum refractive index of the core and n_{clad} is the cladding refractive index.

Combining with the (5), the time delay between two beating modes can be defined as:

$$\Delta t = \frac{L}{c/n_{01}} - \frac{L}{c/n_{02}} = \frac{\Delta n L}{c} = \frac{\lambda^2}{c\Delta\lambda} \quad (7)$$

It shows that the delay time only depends on the effective index difference Δn and the MMF length, L. In order to evaluate the delay efficiency of our proposed all-fiber MZI, we also define another parameter called delay coefficient, Δd, corresponding to the time delay in a one-meter MMF:

$$\Delta d = \frac{\Delta t}{L} = \frac{\Delta n}{c} = \frac{\lambda^2}{cL\Delta\lambda} \quad (8)$$

We can that the delay coefficient only depends on the effective index difference Δn, which is determined by the MMF refractive index profile.

3 EXPERIMENT

According to the theoretical analysis in Section 2, we built an experimental setup, as shown in Fig. 3, for observing the transmission spectrum of our proposed all-fiber MZI. A white source with almost a flat spectrum in the range from 1 μm to 1.62 μm was used as the light source. The SMFs (9 μm /125 μm) were the commercial standard SMFs compliant with ITU-T G.652, and the MMF (50 μm /125 μm) was also a commercial graded-index MMF, with maximum core refractive index of 1.473 and cladding refractive index of 1.4567. In the experiment, the MMF was spliced between two SMFs by two micro-positioners, for accurately adjusting the transverse offset. Note that the micro-positioners are not shown in Figure 3. Finally, the output-SMF was directly connected to an optical spectrum analyzer (OSA) for observing and recording the transmission spectrum.

The experimental results of transmission spectrums are shown in Figure 4, with different MMF lengths of 38.5, 46 and 76 cm. As can be seen, interference ER as high as 18 dB is obtained in the experiment. These results agree with the theory presented in Section 2: most power is coupled into modes LP_{01} and LP_{11}, and power difference between these two modes is small. Also, comparison between Figure 4 (a) and (c) indicates that the transmission spacing $\Delta\lambda$ is inversely proportional to the MMF length: increasing MMF length from 38.5 to 76 cm results in a decrease of wavelength spacing $\Delta\lambda$ from 4.34 to 2.22 nm.

Figure 4(a) also shows that a relative time delay Δt of 1.85 ps, which is got through (7), is obtained when the MMF length is 38.5 cm. According to (8), it can be calculated that the delay coefficient Δd is 4.81 ps/m. This value is larger than that of step-index MMF based MZI (Lize, Gomma and Kashyap, 2006) and birefringent fiber based loop mirror (Chow and Tsang, 2005), which possesses delay coefficients of 3.48 and 0.91 ps/m, respectively. It implies that the required MMF length for generating a certain time delay is much shorter. However, the delay coefficient of our proposed all-fiber MZI device is much smaller than that of all-fiber MZIs proposed by Chen (Chen, Horche and Minguez, 2014) and Du (Du et al., 2010), which possesses delay coefficients of 8.7 and 30.4 ps/m, respectively.

The transmission spectrums in Figures 4(b) and (c) reveal the periodic nature on the change of the interference ER. This phenomenon agrees with the theoretical analysis mentioned in Section 2: some high-order modes, such as modes LP_{02} and LP_{21}, are excited and propagating in the MMF. Note, however, that the transmission spectrum is mainly determined by the phase difference between modes LP_{01} and LP_{11} at the end of MMF. At a certain wavelength, the output power reaches the minimum due to the destructive interference, when the phase

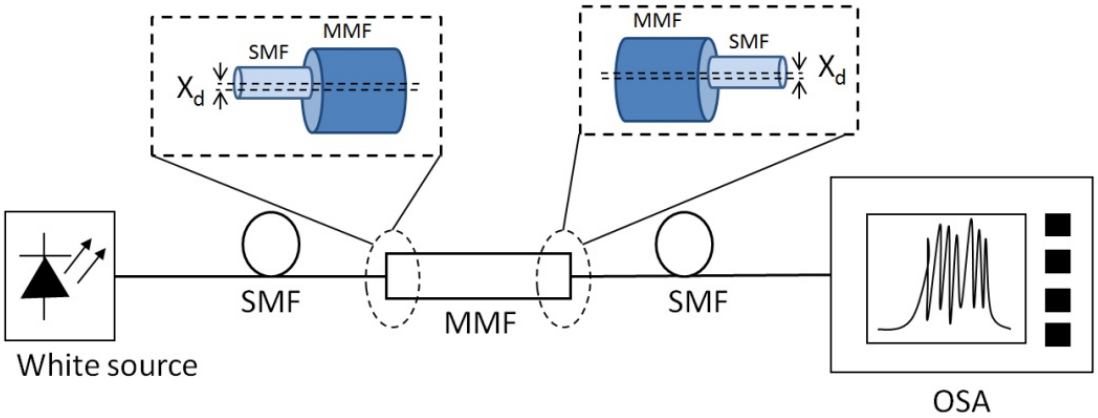

Figure 3: Experimental setup. LED: light emitting diodes; MMF: multimode fiber; SMF: single-mode fiber; OSA: optical spectrum analyzer.

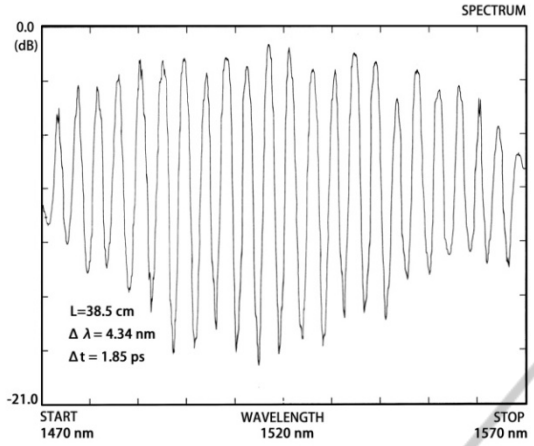

(a)

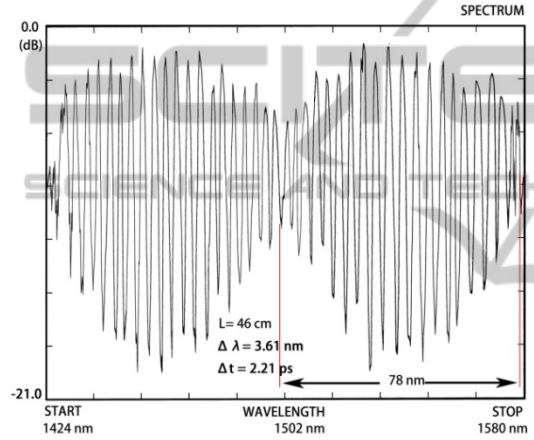

(b)

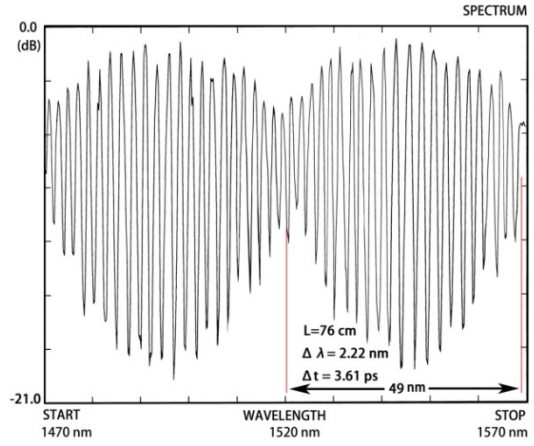

(c)

Figure 4: Transmission spectrum of the all-fiber MZI device with different MMF lengths of 38.5 cm (a), 46 cm (b), and 76 cm (c).

difference is equal to even times of π. In theory, the spectral period should be inversely proportional to MMF length, which agrees with the experimental results: increasing MMF length from 46 cm to 76 cm leads to a decrease of spectral period from 78 nm to 49 nm.

4 PROPOSED MZI FOR DPSK SIGNALS DEMODULATION

As mentioned in Section 1, interference ER is a very important parameter for demodulating DPSK signals, when an all-fiber MZI is used as a DPSK demodulator. The high interference ER obtained in the experiment make our proposed all-fiber MZI device possible for using as a DPSK demodulator. In this section, we verify, through simulation, that our proposed all-fiber MZI can be used for DPSK signals demodulation.

The MMF model used in the simulation is almost the same as the graded-index MMF used in the experiment. It can be theoretically calculated that the delay coefficient is 4.93 ps/m, which is very close to the results obtained in the experiment. The required MMF length, thus, is 5.068m for demodulating a 40Gbps DPSK signal. Figure 5 shows the transmission spectrum of the proposed all-fiber MZI with MMF length of 5.068 m. It can be seen that high interference ER is obtained in the simulation.

Simulation design of a back-to-back 40 Gbps DPSK system, including a conventional transmitter and a receiver based on our proposed all-fiber MZI, is depicted in Figure 6. A the transmitter, a 1550 nm continuous-wave source was modulated by a $LiNbO_3$ Mzch-Zehnder modulator (MZM), driven by a 40 Gbps precoded data stream, which is a pseudo randam bit sequence of length 2^{15}-1, to generate a 40 Gbps DPSK signal. At the receiver, the signal was first amplified by an erbium-doped fiber amplifier (EDFA), and then the noise-loaded signal was filtered by a bandpass filter with an 85-GHz 3-dB bandwidth. After that, the signal was demodulated by our proposed all-fiber MZI, followed by a photodetector. Finally, a bit error rate (BER) analyzer was used to analyze the quality of the received signal. Note that the simulations were carried out through OptiSystem.

The simulation results of back-to-back sensitivity are shown in Figure 7. The sensitivity of our proposed receiver is about -22.5 dBm at a BER of 10-15 and about -23.9 dBm at a BER of 10-9. Compared with the conventional delay interferometer based DPSK receiver built with two fiber couplers (Gnauck and Winzer, 2005), our proposed receiver has 1.3 ± 0.2 dB sensitivity

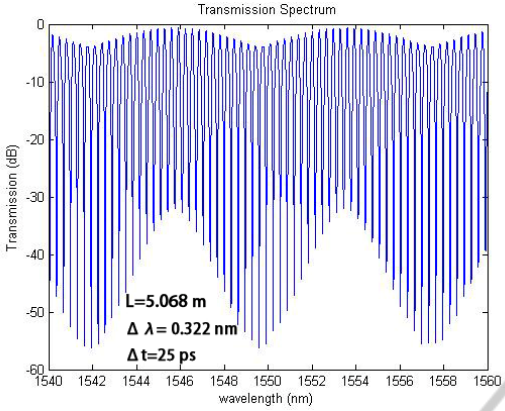

Figure 5: Transmission spectrum of the proposed all-fiber MZI with MMF length of 5.068m.

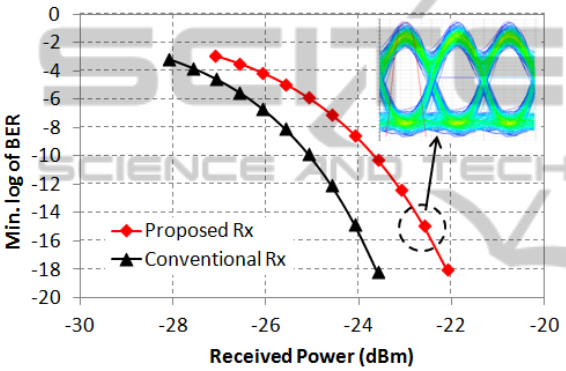

Figure 7: BER as a function of received power.

penalty. This penalty is mainly caused by the imbalanced detection, since the output-SMF only provides one output port. This problem can be solved by splicing a dual-core fiber at the output end of the proposed MZI, thus, detecting the demodulated signals in the two cores. However, it should be noted this design is at the expense of increasing the complexity of the receiver. In addition, the MMF induced signal impairment can also lead to sensitivity penalty. The relatively open intensity eye shown in the inset demonstrates that the proposed receiver can provide error-free operation.

5 CONCLUSIONS

We have demonstrated, through theory and experiment, an all-fiber MZI device, which is based on a commercial graded-index MMF mismatch spliced between two SMFs. In this structure, most of the input power is coupled into modes LP_{01} and LP_{11} excited in the MMF. These two modes interfere with each other along the propagation direction, and the light power coupled into the output-SMF only depends on the relative phase difference at the end of the MMF. Thus, interference pattern can be obtained at the exit of the output-SMF. Interference ER, as high as 18 dB, is obtained in the experiment, and a delay coefficient of 4.81ps/m is obtained also. Finally, simulations of using the proposed all-fiber MZI to demodulate a 40 Gbps DPSK signal are done. Simulation results show that the proposed DPSK receiver has similar performance as the conventional receiver built with two couplers, but with 1.3 ± 0.2 dB sensitivity penalty.

Since the design of our proposed all-fiber MZI is low-cost and easy manufactured, it will be used widely in many optical applications in the future, such as filters or temperature sensors. Moreover, with the proper design, it can also be used as WDM multiplexer and demultiplexer.

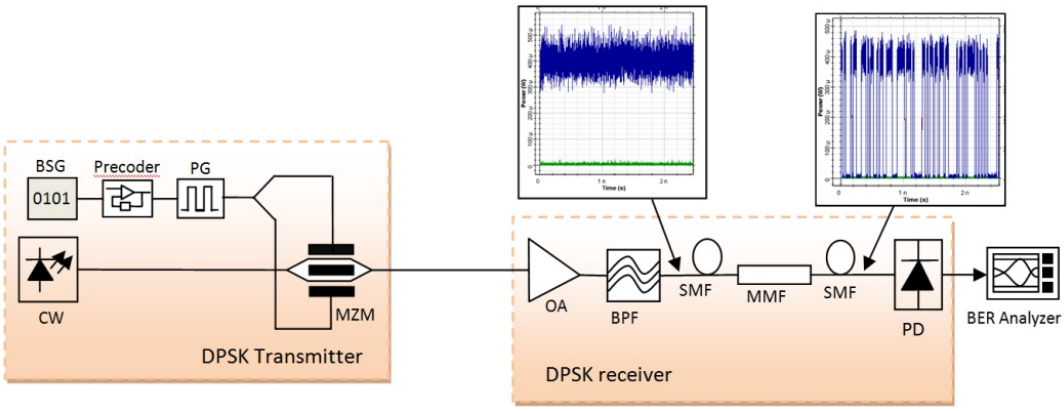

Figure 6: Simulation setup. CW: continuous wave; BSG: bit sequence generator; PG: pattern generator; MZM: Mach-Zehnder modulator; OA: optical amplifier; BPF: bandpass filter; BER: bit error rate; PD: photodetector.

ACKNOWLEDGEMENTS

The authors would like to acknowledge support from the China Scholarship Council (CSC). The authors would also like to dedicate this work to the memory of the recently deceased Professor Alfredo Martín Mínguez.

REFERENCES

Abe, K., Lacroix, Y., Bonnell, L., Jakubczyk, Z., 1992. Modal interference in a short fiber section: fiber length, splice loss, cutoff, and wavelength dependences. *Journal of Lightwave Technology*. vol. 10, no. 4, pp. 401-406.

Blahut, M., Kasprzak, D., 2004. Multimode interference structures – properties and applications. *Optica* Applicata. vol. XXXIV, no.4, pp. 573-587.

Chen, X., Horche, P.R., Minguez, A.M., 2014. DPSK Signals Demodulation Based on a Multimode Fiber with a Central Dip. In *NOC 2014*, Milan, Italy.

Chow, C.W., Tsang, H.K., 2005. Polarization-independent DPSK demodulation using a birefringent fiber loop. IEEE Photonics Technology Letters. vol. 17, no. 6, pp. 1313–1315.

Du, J., Dai, Y., Lei, G.K.P., Tong, W., Shu, C., 2010. Photonic crystal fiber based Mach-Zehnder interferometer for DPSK signal demodulation. *Optics Express*. vol. 18, no. 8, pp. 7917-7922.

Gnauck, A.H., Winzer, P.J., 2005. Optical phase-shift-keyed transmission. *Journal of Lightwave Technology*. vol. 23, no. 1, pp. 115-130.

Hofmann, P., Mafi, A., Jollivet, C., Tiess, T., Peyghambarian, N., Schülzgen, A., 2012. Detailed investigation of mode-field adapters utilizing multimode-interference in graded index fibers. *Journal of Lightwave Technology*. vol. 30, no. 14, pp. 2289-2298.

Horche, P.R., López-Amo, M., Muriel, M.A., Martin-Pereda, J.A., 1989. Spectral behavior of a low-cost all-fiber component based on untapered multifiber unions. *IEEE Photonics Technology Letters*. vol. 1, no. 7, pp. 184-187.

Horche, P.R., Muriel, M.A., Martin-pereda, J.A., 1989. Measurement of transmitted power in untapered multifibre unions: oscillatory spectral behaviour. *Electronics Letters*. vol. 25, no. 13, pp. 843-844.

Kumar, A., Varshney, R.K., Antony, S., Sharma, P., 2003. Transmission characteristics of SMS fiber optic sensor structures. Optics Communications. vol. 219, no. 1-6, pp. 215-219.

Lize, Y.K., Gomma, R., Kashyap, R., 2006. Low-cost multimode fiber Mach-Zehnder interferometer for differential phase demodulation. In *SPIE 2006*, San Diego, USA.

Mohammed, W.S., Mehta, A., Johnson, E.G., 2004. Wavelength tunable fiber lens based on multimode interference. *Journal of Lightwave Technology*. vol. 22, no. 2, pp. 469-477.

Pang, F., Liang, W., Xiang, W., Chen, N., Zeng, X., Chen, Z., and Wang, T., 2009, Temperature-Insensitivity Bending Sensor Based on Cladding-Mode Resonance of Special Optical Fiber, *IEEE Photonics Technology Letters*, vol. 21, no. 2, pp. 76-78.

Shao, M., Qiao, X., Fu, H., Li, H., Jia, Z., Zhou, H., 2014. Refractive index sensing of SMS fiber structure based Mach–Zehnder interferometer. *IEEE Photonics Technology Letters*. vol. 26, no. 5, pp. 437-439.

Tripathi, S.M., Kumar, A., Marin, E., Meunier, J.-P., 2010. Single-multi-single mode structure based band pass/stop fiber optic filter with tunable bandwidth. *Journal of Lightwave Technology*. vol. 26, no. 24, pp. 3535-3541.

Tripathi, S.M., Kumar, A., Varshney, R.K., Kumar, Y.B.P., Marin, E., Meunier, J.-P., 2009. Strain and temperature sensing characteristics of single-mode-multimode-single-mode structures. *Journal of Lightwave Technology*. vol. 27, no. 13, pp. 2348-2355.

Wang, P., Brambilla, G., Ding, M., Semenova, Y., Wu, Q., Farrell, G., 2011. Investigation of single-mode–multimode–single-mode and single-mode–tapered-multimode–single-mode fiber structures and their application for refractive index sensing. *J. Opt. Soc. Am. B*. vol. 28, no. 5, pp. 1180-1186.

Wang, Q., Farrell, G., and Yan, W., 2008. Investigation on single-mode–multimode–single-mode fiber structure. *Journal of Lightwave Technology*. vol. 26, no. 5, pp. 512-519.

Winzer, P.J., Essiambre, R.-J., 2006. Advanced optical modulation formats. Proceedings of the IEEE. vol. 95, no. 5, pp. 952-985.

Xue, L.-L., Yang, L., 2012. Sensitivity enhancement of RI sensor based on SMS fiber structure with high refractive index overlay. *Journal of Lightwave Technology*. vol. 30, no. 10, pp. 1463-1469.

Zhu, J.-J., Zhang, A.P., Xia, T.-H., He, S., and Xue, W., 2010. Fiber-Optic High-Temperature Sensor Based on Thin-Core Fiber Modal Interferometer, *IEEE Sensors Journal*, vol. 10, no. 9, pp. 1415-1418.